Toll-like receptor 4 mediates synergism between alcohol and HCV in hepatic oncogenesis involving stem cell marker Nanog

Keigo Machida[a,b,1], Hidekazu Tsukamoto[a,c,d], Hasmik Mkrtchyan[a], Lewei Duan[b], Alla Dynnyk[a], Helene Minyi Liu[b], Kinji Asahina[a], Sugantha Govindarajan[a,c], Ratna Ray[e], Jing-hsiung James Ou[a,b], Ekihiro Seki[f], Raymond Deshaies[g], Kensuke Miyake[h], and Michael M.-C. Lai[b,i]

[a]Southern California Research Center for Alcoholic, Liver, and Pancreatic Diseases and Cirrhosis, and Departments of [b]Molecular Microbiology and Immunology and [c]Pathology, University of Southern California, Keck School of Medicine, 2011 Zonal Avenue, Los Angeles, CA 90033; [d]VA Greater Los Angeles Healthcare System, Los Angeles, CA 90033; [e]Department of Pathology, Saint Louis University, St. Louis, MO 63103; [f]University of California at San Diego, La Jolla, CA 92093; [g]Howard Hughes Medical Institute and Division of Biology, California Institute of Technology, Pasadena, CA 91125; [h]Institute of Medical Science, University of Tokyo, Tokyo 108-8639, Japan; and [i]Department of Microbiology and Immunology, National Cheng Kung University, Tainan 701, Taiwan

Edited by Peter Palese, Mount Sinai School of Medicine, New York, NY, and approved December 2, 2008 (received for review August 13, 2008)

Alcohol synergistically enhances the progression of liver disease and the risk for liver cancer caused by hepatitis C virus (HCV). However, the molecular mechanism of this synergy remains unclear. Here, we provide the first evidence that Toll-like receptor 4 (TLR4) is induced by hepatocyte-specific transgenic (Tg) expression of the HCV nonstructural protein NS5A, and this induction mediates synergistic liver damage and tumor formation by alcohol-induced endotoxemia. We also identify Nanog, the stem/progenitor cell marker, as a novel downstream gene up-regulated by TLR4 activation and the presence of CD133/Nanog-positive cells in liver tumors of alcohol-fed NS5A Tg mice. Transplantation of p53-deficient hepatic progenitor cells transduced with TLR4 results in liver tumor development in mice following repetitive LPS injection, but concomitant transduction of Nanog short-hairpin RNA abrogates this outcome. Taken together, our study demonstrates a TLR4-dependent mechanism of synergistic liver disease by HCV and alcohol and an obligatory role for Nanog, a TLR4 downstream gene, in HCV-induced liver oncogenesis enhanced by alcohol.

Chronic liver damage caused by viral infection, alcohol, metabolic syndrome, or these factors in combination can increase the risk for hepatocellular carcinoma (HCC), which is the fifth most common cancer in the world (1). In particular, chronic infection with hepatitis B virus (HBV) or hepatitis C virus (HCV) represents a major risk factor for HCC (1). HCV infects more than 170 million people worldwide (1–3). Ample epidemiological evidence suggests that there is a strong connection between HCV and alcoholic liver disease (ALD). First, the prevalence of HCV infection is significantly higher among alcoholics than in the general population (4). Second, the presence of HCV infection correlates with the severity of the disease in alcoholic subjects, as such that HCV-infected patients with ALD develop liver cirrhosis and HCC at significantly accelerated rates than do uninfected ALD patients, suggesting that alcohol and HCV work synergistically to cause liver damage (5). Several possible mechanisms may explain the high prevalence of HCV among alcoholics and the increased severity of liver diseases in these patients. Alcohol may enhance the replication of HCV and increase the expression of viral RNA and proteins, resulting in more severe HCV-induced liver injury, and this may in part explain a positive correlation between HCV titer and the amount of alcohol consumption (6). A metabolite and metabolic side-products of ethanol, such as acetaldehyde and free radicals, may directly stimulate HCV replication and gene expression (7, 8). Enhanced HCV replication may also be indirectly caused by alcohol-induced immunosuppression (9).

Recent studies with mice expressing HCV proteins have shed pivotal insight into the mechanisms underlying the synergism with alcohol. The HCV core protein causes overproduction of reactive oxygen species, which appears to be responsible for mitochondrial DNA damage (10). The core protein also inhibits microsomal triglyceride transfer protein activity and very low-density lipoprotein (VLDL) secretion (11), which may underlie the genesis of fatty liver. The core protein also induces insulin resistance in mice and cell lines, and this effect may be mediated by degradation of insulin receptor substrates (IRS) 1 and 2 via up-regulation of SOCS3 (12) in a manner dependent on PA28γ 73 or via IRS serine phosphorylation (13). Thus, these core-induced perturbations, such as oxidant stress and insulin resistance, which are also known risk factors for ALD, may contribute to the synergism reproduced in alcohol-fed core transgenic mice (14).

The most devastating consequence of the synergism between viral hepatitis and alcohol is HCC (15–19). The risk of developing HCC as assessed by odds ratio increases from 8 to 48 by having concomitant alcohol abuse in HCV- and/or HBV-infected patients (19). Although the effects of the core described above may contribute to this synergism, we directed our attention to the HCV nonstructural protein NS5A as a potential effector for the synergism. NS5A is known to have a cryptic *trans*-acting activity for cellular gene promoters (20) and to interact with an IFN-induced, double-stranded RNA-activated protein kinase PKR (21), thus accounting for the resistance of most HCV strains to IFN treatment. Our recent study revealed that NS5A expression induces TLR4 in the B cell lymphoma cell line Raji and the hepatoma cell line Huh7 (22). This result raised a possibility that NS5A-induced TLR4 may aggravate ALD, which is known to be mediated by endotoxin, the ligand for TLR4. Indeed, the present study provides direct mechanistic evidence that hepatocyte-specific transgenic (Tg) expression of the HCV nonstructural protein NS5A up-regulates TLR4, which in turn induces severe steatohepatitis and liver tumors when this pattern recognition receptor is activated by alcohol-induced endotoxemia. Further, our research identifies the stem cell marker Nanog as a direct downstream gene required for TLR4-dependent liver oncogenesis.

Results

NS5A Induces TLR4 Expression in the Mouse Liver. We have shown previously that NS5A induces the expression of TLR4 in the B cell

Author contributions: K. Machida, H.T., R.R., J.-h.J.O., R.D., and M.M.-C.L. designed research; K. Machida, H.T., H.M., L.D., A.D., H.M.L., K.A., S.G., and E.S. performed research; K. Machida, R.R., and K. Miyake contributed new reagents/analytic tools; K. Machida analyzed data; and K. Machida, H.T., J.-h.J.O., and M.M.-C.L. wrote the paper.

The authors declare no conflict of interest.

This article is a PNAS Direct Submission.

[1]To whom correspondence should be addressed. E-mail: kmachida@usc.edu.

This article contains supporting information online at www.pnas.org/cgi/content/full/0807390106/DCSupplemental.

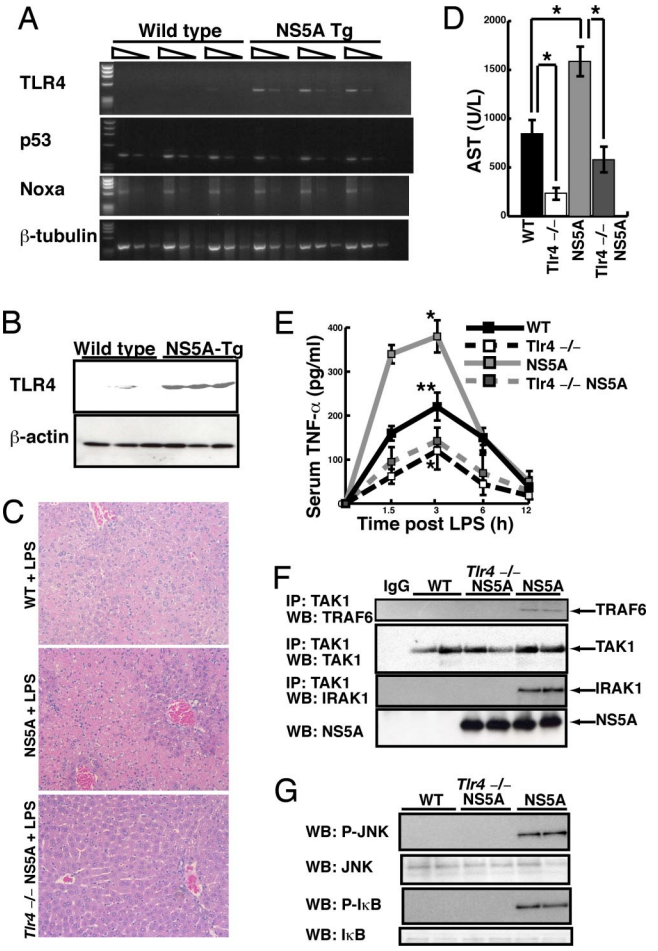

Fig. 1. Increased susceptibility of NS5A transgenic mice to endotoxin challenge. (*A* and *B*) TLR4 mRNA and protein expressions in the liver of NS5A Tg mice were increased, as demonstrated by RT-PCR (*A*) and Western blot (*B*) analyses. (*C*) H&E-stained sections of livers collected 24 hours after LPS challenge (25 mg/kg weight, intraperitoneally) showed coagulative necrosis with hemorrhage in NS5A Tg mice (*Middle*) but no histological abnormality in wild-type mice (WT, *Top*) or NS5A Tg mice with TLR4 deficiency (Tlr4$^{-/-}$NS5A, *Bottom*) (Magnification: 100×). (*D*) Serum AST levels at 24 hours after LPS challenge. TLR4 deficiency (Tlr4$^{-/-}$) attenuated LPS-induced elevation of AST compared with wild-type mice (WT; *, $P < 0.05$). NS5A Tg mice showed an augmented AST elevation compared with WT (*, $P < 0.05$), and this effect was abrogated by TLR4 deficiency (Tlr4$^{-/-}$NS5A) (*, $P < 0.05$). (*E*) Time course changes in serum TNF-α level after LPS injection. Increased TNF-α levels in WT were reduced in Tlr4$^{-/-}$ (*, $P < 0.05$) but augmented in NS5A mice (**, $P < 0.05$). Heightened TNF-α levels in NS5A mice were abrogated in Tlr4$^{-/-}$NS5A (***, $P < 0.05$). (*F*) LPS-induced signaling, such as TAK1 interaction with TRAF6 or IRAK, was enhanced in NS5A but not Tlr4$^{-/-}$NS5A mice. (*G*) LPS-induced phosphorylation of JNK and IκBα in the liver was increased in NS5A but not Tlr4$^{-/-}$NS5A mice.

lymphoma cell line Raji and the hepatoma cell line Huh7 (22). However, whether NS5A induces TLR4 in the liver of the whole animal is yet to be determined. To address this question, NS5A was expressed in a hepatocyte-specific manner in mice with the use of an apoE promoter (23, 24). RT-PCR and immunoblot analyses confirmed induction of TLR4 mRNA and protein levels in the NS5A Tg mouse liver compared with the wild-type (WT) mouse liver (Fig. 1 *A* and *B*). Expressions of p53, Noxa, and β-tubulin mRNA were not different between the 2 groups (25, 26). These results demonstrate in vivo induction of hepatic TLR4 expression by NS5A and support the rationale for testing the role of TLR4 in synergistic liver damage by alcohol and HCV NS5A.

LPS Induces Fulminant Hepatitis and Mortality in NS5A Tg Mice in a TLR4-Dependent Manner. To test the functionality of NS5A-induced TLR4, we created 4 genetic mouse lines with the identical background C57BL/6: (*i*) WT mice (WT); (*ii*) WT mice with TLR4 deficiency (Tlr4$^{-/-}$); (*iii*) NS5A Tg mice (NS5A); and (*iv*) NS5A Tg mice with TLR4 deficiency (Tlr4$^{-/-}$NS5A). These mice were challenged by intraperitoneal injection of an acute sublethal dose of LPS (25 mg/kg). This challenge expectedly and markedly raised the serum levels of aspartate aminotransferase (AST) and TNF-α in WT, whereas these parameters were significantly attenuated in Tlr4$^{-/-}$ (Fig. 1 *D* and *E*). LPS-challenged WT mice did not show conspicuous liver pathology (Fig. 1*C Top*) or mortality [supporting information (SI) Fig. S1*A*]. In contrast, in NS5A Tg mice, LPS caused 30% mortality (Fig. S1*A*), fulminant hepatitis characterized by massive hemorrhagic liver necrosis and inflammation (Fig. 1*C Middle*), and augmented elevations of serum AST and TNF-α (Fig. 1 *D* and *E*). Importantly, all of these changes were largely abrogated in Trl4$^{-/-}$NS5A mice (Fig. 1 *C–E* and Fig. S1*A*), supporting the role of TLR4 in LPS-induced hepatitis and mortality in NS5A mice. Next, we validated whether NS5A expression augmented LPS-induced signal transduction via TLR4 by assessing the interaction of TGF-α-activated kinase 1 (TAK1) with TNFR-associated factor 6 (TRAF6) or IL-1 receptor-associated kinase-1 (IRAK1), the signaling events immediately downstream of LPS-TLR4-CD14 binding (13). Coimmunoprecipitation analysis of liver protein extracts readily detected enhanced TAK1–TRAF6 and TAK1–IRAK1 interactions in NS5A mice given LPS, whereas these protein–protein interactions were not observed in WT or Tlr4$^{-/-}$NS5A mice under the same immunoblotting condition (Fig. 1*F*). We also analyzed phosphorylation of JNK and IκBα, 2 further downstream parameters of TLR4 signaling. As shown in Fig. 1*G*, phosphorylation of JNK and IκBα (*p*-JNK, p- IκBα) was also prominent in NS5A mice but not in WT or Tlr4$^{-/-}$NS5A mice (Fig. 1*G*). These results demonstrate augmented activation of TLR4 signaling in the liver of LPS-challenged NS5A mice and their sensitization for LPS-induced fulminant hepatitis.

Because TLR4 was primarily induced in hepatocytes by hepatocyte-specific expression of NS5A, the accentuated liver damage in NS5A mice is presumed to have resulted from heightened TLR4 activation in the parenchymal cells. However, Kupffer cells still represent another obvious cellular site of TLR4 signaling. Thus, to determine whether or to what extent Kupffer cells contribute to liver injury induced by LPS in NS5A mice, we depleted Kupffer cells by administration of liposome-encapsulated Clodronate (27) 2 days before LPS injection. This method depletes more than 95% of Kupffer cells (27) and largely (75≈80%) prevented LPS-induced increases in serum AST and TNF-α levels in WT, confirming that Kupffer cells are the predominant site of TLR4 activation. In NS5A, however, the same manipulation reduced these parameters only by 35% and 39%, respectively (Fig. S1 *B* and *C*) and did not attenuate the mortality rate (data not shown). From these results, we conclude that Kupffer cell-derived TNF-α accounted for ≈40% of total TNF-α produced in response to LPS in NA5A mice and had a only minor if no role in liver damage and mortality in this model. Conversely, these results suggest that the remaining 60% of TNF-α in the serum of these mice was produced by TLR4-expressing hepatocytes.

Expression of NS5A and TLR4 in Hepatitis C Patient Livers. Next, we assessed the clinical relevance of our finding on TLR4 induction in NS5A mice. Liver protein extracts were obtained from healthy subjects, patients with HCV infection, and HCV patients with a history of alcoholism. These samples and the samples from NS5A mouse livers were concomitantly analyzed for the expression of NS5A by immunoblot analysis. As shown in Fig. S2*A*, the expression of NS5A is increased in HCV patients with or without alcoholism compared with healthy subjects. A densitometric anal-

ysis of normalized NS5A expression shows that the expression in the patient livers is about a third of the level seen in NS5A mice (Fig. S2*B*). These results indicate that NS5A Tg expression in our mouse model is not extremely unphysiological. Next, we performed immunocytochemistry on liver cryosections from HCV patients with or without alcoholism to assess the expression of TLR4 and 2 downstream parameters of TLR4 signaling: *p*-JNK and *p*-IκBα. In these samples, increased colocalization of TLR4 with *p*-JNK and *p*-IκBα was noted, particularly in HCV patients with alcoholism (Fig. S2 *D* and *E*). These results support the clinical relevance of our finding on TLR4 induction and activation in NS5A mice.

NS5A-Induced TLR4 Aggravates Alcoholic Steatohepatitis. Because NS5A mice are sensitive to LPS due to TLR4 induction, and alcohol-induced liver injury is known to be mediated by endotoxin, we tested whether NS5A Tg mice are more susceptible to alcohol-induced liver damage. For this, the same 4 genetic lines of mice described above (WT, Tlr4$^{-/-}$, NS5A, and Tlr4$^{-/-}$NS5A) were fed either control or ethanol diet by intragastric infusion that allowed maximal ethanol intake for 4 weeks (see experimental design in Fig. S3*A*). Ethanol feeding in WT mice resulted in diffuse (2+≈4+) fatty liver with or without small foci of inflammation (Table S1) and a 2.7-fold increase in plasma alanine aminotransferase (ALT) levels (95 ± 18 units/L) compared with control diet-fed WT mice (Fig. S3*B*). In contrast, ethanol-fed NS5A Tg mice displayed an additional 2-fold increment in ALT elevation (181 ± 21 units/L) compared with ethanol-fed WT mice (Fig. S3*B*). Spotty and submassive liver necrosis, as well as infiltration of mononuclear cells, neutrophils, and eosinophils in the necrotic midzone region, was also observed in these mice (Fig. S3*G*). This pathology resembles coagulative necrosis commonly observed in chronically ethanol-fed rodents given acute LPS and confirmed that NS5A Tg mice are more susceptible to alcoholic steatohepatitis. This pathology and the elevation of the plasma ALT level were largely abolished in Tlr4$^{-/-}$NS5A mice (Table S1 and Fig. S3 *D* and *H*), confirming the pathogenic role of TLR4 in this mouse model. It should be noted that the plasma endotoxin levels in NS5A Tg and WT mice were equally elevated by alcohol feeding compared with pair-fed control animals (Fig. S3*C*).

Next, we determined the role of endotoxin in alcoholic steatohepatitis in NS5A Tg mice by intragastric administration of polymyxin B (150 mg/kg per day) and neomycin (450 mg/kg per day) for 4 days before alcohol feeding and during the entire feeding period. This antibiotic treatment reduced ALT levels (Fig. S3*E*) and liver pathology in ethanol-fed NS5A Tg mice (Fig. S3*I* and Table S1). Conversely, LPS was administered weekly via the intragastric tube to ethanol-fed NS5A Tg mice to test whether this manipulation accentuates alcoholic liver damage. As expected, LPS aggravated liver damage caused by alcohol (Table S1) and led to 2.5-fold higher serum ALT levels compared with alcohol-fed NS5A mice without LPS (Fig. S3*E*). These results indicate the importance of endotoxin-activated TLR4 signaling in the pathogenesis of aggravated steatohepatitis in alcohol-fed NS5A Tg mice. Oxidant damage is a key feature of alcoholic liver damage that can be further potentiated by endotoxin (28, 29). Thus, we measured the hepatic content lipid peroxides in WT and NS5A Tg mice fed alcohol or control diet. Alcohol feeding increased the lipid peroxide levels 2-fold in WT mice. In NS5A Tg mice, this effect was significantly accentuated with a 3.3-fold elevation, indicating enhanced oxidative damage in alcohol-fed NS5A Tg mice (Fig. S3*J*).

NS5A-Induced TLR4 Causes Synergistic Liver Oncogenesis by Long-Term Alcohol Feeding. We next extended our study to determine whether NS5A-mediated TLR4 induction causes liver tumor after prolonged alcohol feeding. For this experiment, we fed the same 4 genetic lines of mice Lieber-DeCarli diet containing 3.5% (wt/vol) ethanol or isocaloric dextrin for 12 months. This liquid diet containing the lower ethanol concentration was fed ad libitum, and this

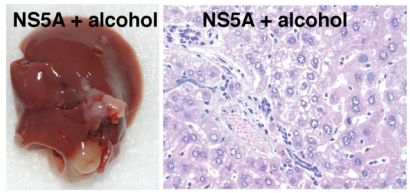

Fig. 2. HCV NS5A induced liver tumors after 12-month alcohol feeding, as shown in this representative photograph (*Left*) of gross liver appearance and a microphotograph (*Right*) of an H&E-stained section of the tumor. (Magnification: 100×).

regimen alleviated the high mortality commonly associated with this type of long-term feeding. Total daily caloric intakes from the control or ethanol diet by different genetic groups were not significantly different (WT: 17.2 ± 3.4 vs. 15.3 ± 2.8, Tlr4$^{-/-}$: 18.1 ± 3.1 vs. 16.1 ± 4.4, NS5A: 18.1 ± 4.1 vs. 15.7 ± 3.0, and Tlr4$^{-/-}$NS5A: 17.6 ± 3.6 vs. 16.3 ± 4.0 mL/mouse per day). Liver tumor was not detected in WT, NS5A Tg, or Tlr4$^{-/-}$NS5A mice fed the control diet or WT mice fed the alcohol diet. In contrast, liver tumor was found in 23% of ethanol-fed NS5A Tg mice (Fig. 2 and Table S2) but was completely absent in Tlr4$^{-/-}$NS5A Tg mice (Table S2). Most tumors detected in NS5A mice were hepatoma (Fig. 2). WT and NS5A mice studied for this experiment had relatively even sex distributions (49% and 55% females vs. 51% and 45% males), and the tumor incidence was not statistically different between the 2 sexes (Table S3). Alcohol feeding increased serum TNF-α levels 4-fold in WT mice and 6-fold in NS5A Tg mice, and this difference was significant (Table S2). TLR4 deficiency significantly and largely attenuated this increment in alcohol-fed NS5A mice (Table S2). Enhanced TLR4 signaling by NS5A and alcohol feeding was validated by increased TAK1 interaction with TRAF6 and by elevated *p*-JNK and *p*-IκB in the livers of alcohol-fed NS5A mice but not alcohol-fed WT or Tlr4$^{-/-}$NS5A mice (Fig. S4 *A* and *B*). Colocalization of TLR4 with TNF-α, *p*-IκB, and *p*-JNK was also evident in liver sections of alcohol-fed NS5A but not WT mice (Fig. S4 *C* and *D*). These data demonstrate that alcohol and NS5A synergistically induce liver tumors through enhanced expression of TLR4 and signaling.

Nanog as a TLR4 Downstream Gene Induced by NS5A and Alcohol. To understand the molecular mechanisms of the synergism demonstrated in alcohol-fed NS5A mice, we performed microarray analysis on RNA samples extracted from non-tumor-bearing portions of liver tissues from NS5A Tg and WT mice fed alcohol as described in detail in *SI Methods*. Of more than 39,000 transcripts and variants examined by using more than 45,000 probe sets, 83 transcripts showed increased expression with a cutoff value of 4.0-fold (balanced differential expression) in NS5A mouse livers. The lists of differentially regulated genes are shown in Fig. S5. Of note are induction of a stem cell marker (i.e., Nanog), TLR4 downstream cytokines (e.g., IFN-α4), and apoptosis-related genes (e.g., Bcl2a1a and Bcl11a) as well as down-regulation of the epigenetic transcriptional regulator trithorax group of proteins (e.g., ASH1 and ASH2) and developmental transcription factors (e.g., Hox, Myo, and Fox families).

Induction of the stem cell marker Nanog in alcohol-fed NS5A mice was intriguing in light of the report that a particularly poor prognostic subtype of human HCC is derived from hepatic progenitor cells (30). This induction was confirmed by immunofluorescence microscopy (Fig. 3*A*), immunoblotting (Fig. 3*B*), and quantitative RT-PCR (Fig. 3*C*). Nanog was colocalized with another stem cell marker, CD133 or CD49f, in liver tumors of NS5A Tg mice fed alcohol (Fig. 3*A*), suggesting the presence of cancer stem cells. Nanog induction was dependent on NS5A and alcohol (Fig. 3 *B* and *C*) and abrogated in Tlr4$^{-/-}$NS5A mice fed alcohol

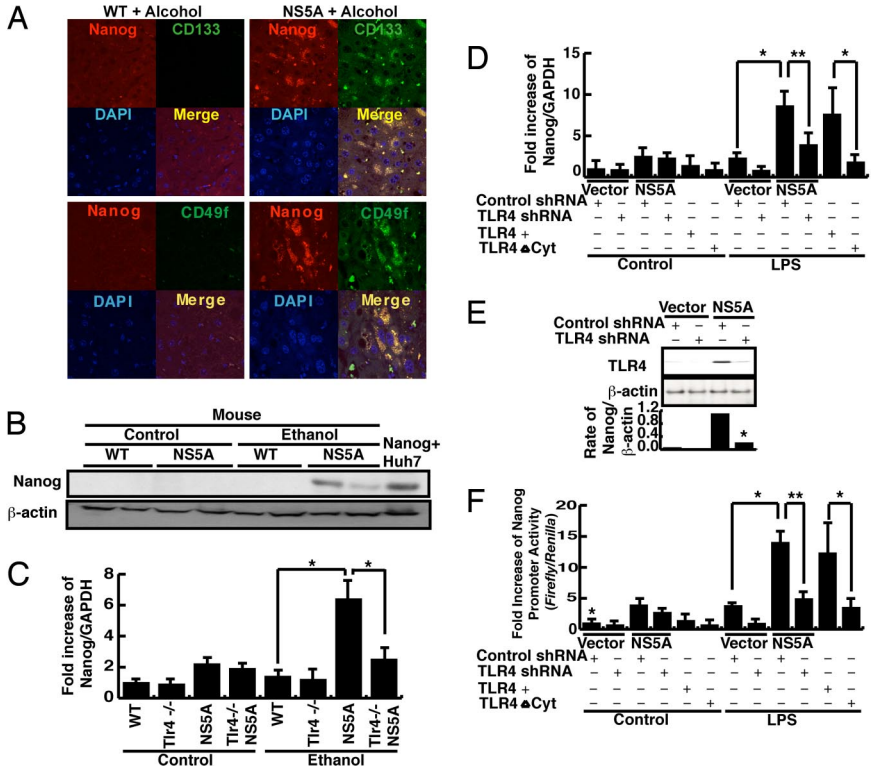

Fig. 3. (*A*) Confocal immunofluorescent microscopy demonstrates colocalization of the stem cell marker Nanog with CD133 or CD49f in the tumor-bearing tissue from NS5A mice fed alcohol for 12 months. (Magnification: 100×.) (*B*) Nanog protein was induced in the livers of NS5A mice fed alcohol, as determined by immunoblot analysis. Immunoblotting of β-actin served as a loading control. (*C*) Nanog mRNA was induced in the livers of NS5A mice fed ethanol, as determined by real-time PCR (*, $P < 0.03$ compared with ethanol-fed WT mice). This induction was attenuated in ethanol-fed Tlr4$^{-/-}$NS5A mice (*, $P < 0.03$ compared with ethanol-fed NS5A). (*D*) LPS induced Nanog mRNA in Huh7 cells transduced with an NS5A expression vector (*, $P < 0.002$ compared with the cells transduced with the empty vector and control shRNA). This induction was suppressed by retroviral expression of shRNA for TLR4 (**, $P < 0.05$). Nanog mRNA also was induced by LPS treatment in the cells transduced with a retroviral vector expressing wild-type TLR4 (TLR4+, *, $P < 0.05$ compared with the control cells), but not in the cells transduced with the mutant TLR4 vector (TLR4ΔCyp). (*E*) Efficient knockdown of TLR4 with the retroviral shRNA vector is evident in this immunoblot analysis and densitometric analysis revealing an 82% reduction (*, $P < 0.05$). (*F*) LPS added to the culture activated the Nanog promoter in Huh7 cells transfected with the promoter-luciferase construct (*, $P < 0.002$ compared with the control cells). TLR4 knockdown with shRNA as above abrogated the promoter activation (**, $P < 0.05$). Expression of wild-type TLR4 (TLR4+, *, $P < 0.05$) but not mutant TLR4 (TLR4ΔCyp) conferred the cells LPS-induced Nanog promoter activation. Relative light unit values were normalized by the activity of the *Renilla* luciferase construct driven by SV40 promoter as a transfection control.

(Fig. 3*C*). We next tested the direct relationship of Nanog induction with TLR4 activation by analyzing Nanog expression in LPS-treated Huh7 cells transduced with an NS5A or control vector with or without TLR4 knockdown with short-hairpin RNA (shRNA). As shown in Fig. 3*D*, LPS up-regulated Nanog expression in NS5A-transduced cells but not in control vector-transfected cells. This induction of Nanog by LPS was significantly reduced by shRNA directed against TLR4 but not by scrambled shRNA (Fig. 3*D*). To assess the efficiency of TLR4 knockdown, we performed immunoblot analysis. As shown in Fig. 3*E*, induction of TLR4 protein by NS5A was decreased approximately by 80% with TLR4 shRNA. Overexpression of Tlr4 (TLR4+) but not the mutant with deletion of the cytoplasmic domain (TLR4ΔCyt) in Huh7 cells also increased the expression of Nanog in the presence of LPS, further validating that activated TLR4 enhances Nanog expression (Fig. 3*D*). To determine whether NS5A induces Nanog expression via TLR4 at the transcriptional level, we performed a reporter assay using a Nanog promoter. LPS treatment increased the reporter activity in the cells transduced with NS5A. This induction was attenuated with TLR4 shRNA but not with control shRNA (Fig. 3*F*). Transduction of wild-type TLR4 but not the mutant TLR4 also caused the promoter activation in the presence of LPS. These results demonstrate that the promoter of the Nanog gene is directly activated by TLR4, and Nanog is a novel downstream gene of TLR4 signaling.

Nanog Mediates TLR4-Dependent Liver Oncogenesis by Hepatic Progenitor Cells. To further validate the role of TLR4 and Nanog in liver oncogenesis in the whole animal, we used the hepatic progenitor cell transplantation model (31). Hepatoblasts were isolated from p53-deficient embryonic livers (embryonic days 12.5≈15), infected with a retroviral vector expressing TLR4 or Nanog along with GFP, and transplanted into wild-type mice via splenic injection. These recipient mice were injected with 3 doses of the hepatotoxin CCl_4 to stimulate reconstitution of transplanted progenitor cells in the liver and were subsequently treated by repetitive intraperitoneal injection of LPS or PBS 3 times a week for 25 weeks (Fig. 4*A*). The cells transduced with a c-myc expression vector served as a positive control, which led to consistent liver tumor formation (Fig. 4 *B* and *C*). Mice receiving a transplant of TLR4-transduced progenitor cells developed liver tumors after 48–54 days following transplantation only when LPS was administered (Fig. 4 *B* and *C*), as judged by GFP imaging of the animals (Fig. 4*D*) and autopsy. No tumor was observed in mice receiving a transplant of the cells transduced with the TLR4 deletion mutant of cytoplasmic domain (ΔCyt), even after LPS injection (Fig. 4*C*). The tumor incidence caused by TLR4 transduction and LPS injection was reduced by coexpression of shRNA against Nanog but not scrambled shRNA (Fig. 4 *B* and *C*). Direct Nanog transduction in hepatic progenitor cells also produced liver tumors, but to a lesser extent compared with the LPS-injected mice with transplantation of TLR4-transduced cells (Fig. 4 *B* and *C*, TLR4 + LPS). The mortality of the mice in the different treatment groups roughly correlated with the liver tumor incidence (Fig. 4*E*).

To further assess the appearance and growth rate of tumors caused by the TLR4- or Nanog-transduced progenitor cells, the cells were injected s.c. into nude mice, and GFP imaging was performed for quantitative assessment of the tumor volume every 8 days for 88 days. TLR4-transduced cells began to form a tumor mass at 40 days after transplantation only when LPS was administered and the cells were deficient in *p53* (*p53*$^{-/-}$), but not when PBS was given or the transplanted cells were from the wild-type mice (*p53*$^{+/+}$) (Fig. 4*F*). The cells transduced with the mutant TLR4 (ΔCyt) did not form tumors. The tumor mass in the TLR4 plus LPS mice steadily grew in size and was approximately half of that seen with c-Myc-transduced cells at the terminal point (Fig. 4*F*). Nanog-

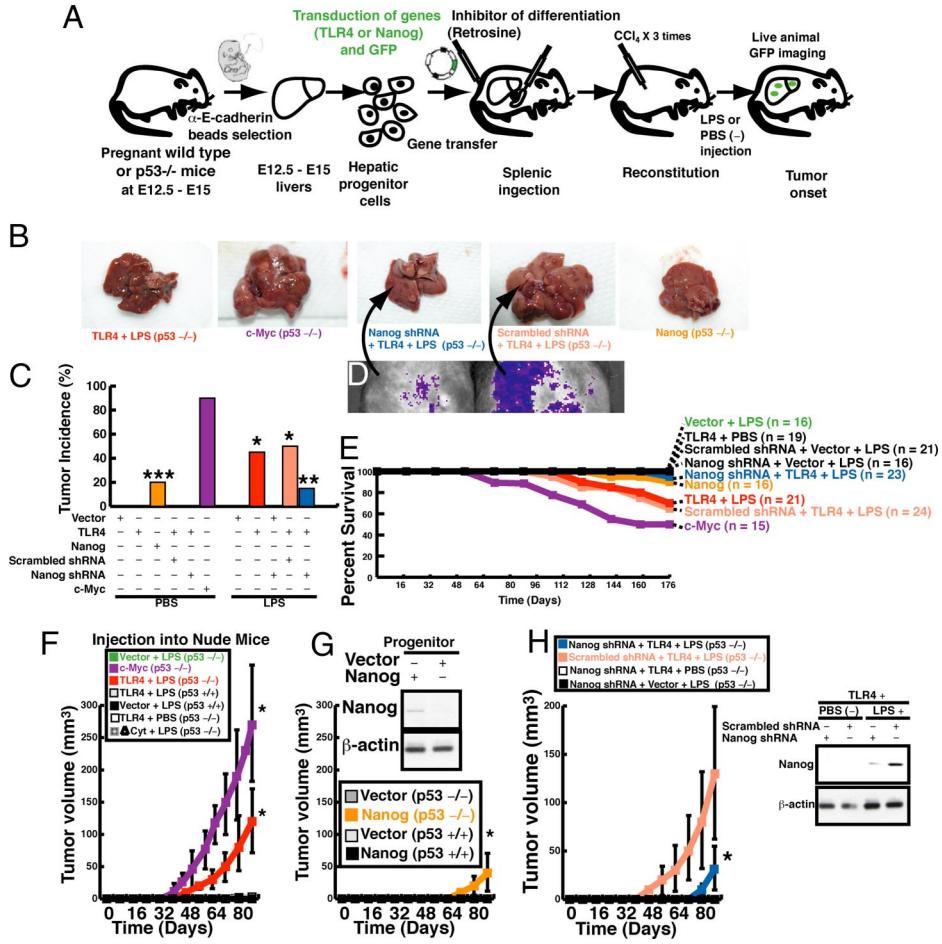

Fig. 4. TLR4-dependent development of liver tumors by hepatoblast transplantation. (*A*) A schematic diagram depicting the generation of liver tumors following retroviral transduction of TLR4 in purified E-cadherin$^+$ hepatoblasts from $p53^{-/-}$ mice, transplantation and engraftment of the hepatoblasts in a recipient C57BL/6 mouse, and repetitive LPS injection. (*B*) Gross photographs of livers following transplantation of $p53^{-/-}$ hepatoblasts transduced with c-Myc, Tlr4, Nanog, shRNA for Nanog, or scrambled shRNA and 25 weeks of LPS treatment (2 mg/kg, intraperitoneally, every other day, the mice with c-Myc-transduced cells did not receive LPS). (*C*) Tumor incidence of recipient mice after transplantation of $p53^{-/-}$ hepatoblasts transduced with the indicated gene and/or shRNA. Mice that were received a transplant of $p53^{-/-}$, c-Myc-transduced cells mostly developed liver tumors without LPS treatment. The mice receiving a transplant of TLR4-transduced $p53^{-/-}$ cells also developed liver tumors at the incidence rate of 40% (*$P < 0.03$). This tumor incidence was suppressed by cotransduction of Nanog shRNA but not control scrambled shRNA (**, $P < 0.05$ compared with the cells transduced with control shRNA). Transduction of Nanog without LPS injection also produced liver tumors, but with much less frequency (***, $P < 0.05$ compared with empty vector-transduced cells without LPS). (*D*) GFP imaging of the tumor-bearing livers of LPS-treated mice transplanted with $p53^{-/-}$ hepatoblasts transduced with TLR4 plus Nanog shRNA or control shRNA. (*E*) Survival curves of mice after transplantation of the cells transduced with the indicated gene and/or shRNA. (*F*) Tumor volume measurement was performed by 3-dimensional GFP imaging of nude mice at various times following s.c. transplantation of $p53^{-/-}$ hepatoblasts transduced with TLR4, a deletion mutant of cytoplasmic domain of TLR4 (ΔCyt), or c-Myc. Note a progressive tumor growth with the c-Myc-transduced cells even without LPS treatment serving as a positive control. Liver tumors arose and grew in mice receiving a transplant of TLR4-transduced cells in response to repetitive LPS injection but not without LPS injection. The cells transduced with the mutant TLR4 failed to form a tumor mass. (*, $P < 0.05$ compared with empty vector-transduced cells with LPS.) (*G*) Hepatoblasts ($p53^{-/-}$) transduced with a Nanog or control retrovirus were subcutaneously transplanted into nude mice, and the tumor mass growth was monitored as above. Immunoblot analysis was performed on the transduced cells after 10 days following infection and just before transplantation. This analysis confirms the expression of Nanog (*Inset*). Nanog-transduced progenitor cells led to a small but significantly increased tumor mass compared with the cells transduced with the control vector (*, $P < 0.05$). (*H*) Hepatic progenitor cells expressing TLR4 gave rise to growing tumors in nude mice repetitively injected with LPS, and this growth was significantly attenuated with Nanog shRNA (*, $P < 0.04$). Immunoblotting of lysates from the hepatoblasts collected 10 days after the transplantation and LPS injection confirms induction of Nanog in TLR4-transduced cells and effective knockdown of Nanog by cotransduction of the specific shRNA (*Inset*).

transduced cells formed a detectable tumor mass in the absence of p53, but at a later time point and with a lesser growth rate (Fig. 4*G*). To determine whether Nanog expression induced by TLR4 signaling is essential for tumor formation and growth in this model, shRNA for Nanog was cotransduced with the TLR4 expression vector. The tumor mass appearance and growth by TLR4-trasnduced, $p53^{-/-}$ progenitor cells were significantly delayed by Nanog shRNA compared with those with scrambled shRNA (Fig. 4*H*). Silencing of Nanog was confirmed by immunoblot analysis of the cells collected 10 days after transplantation (Fig. 4*H Inset*). These results indicate that Nanog mediates the oncogenic potential of activated TLR4, but it alone does not confer the full oncogenic effect.

Discussion

The present study reveals several novel findings with respect to the molecular mechanism underlying synergistic liver pathology caused by HCV and alcohol. First, it demonstrates that NS5A and alcohol synergistically induce hepatocellular damage and transformation via accentuated and/or sustained activation of TLR4 signaling, which results from HCV NS5A-induced TLR4 and endotoxemia associated with alcohol consumption. Second, Nanog is identified as a novel downstream gene transcriptionally induced by activated TLR4 signaling. Third, this stem cell marker is largely responsible for TLR4-mediated liver tumor development, as shown by our hepatic progenitor cell transplantation experiments. Last, despite the common understanding that TLR4 is one of the pattern recognition receptors expressed predominantly by innate immune cells, such as macrophages and lymphocytes, our study demonstrates that hepatocytes can be the primary cellular site of both TLR4 up-regulation and its pathologic consequences in the context of HCV infection. Our experiment with Kupffer cell depletion shows a reduction of serum TNF-α levels by 80% in WT mice but only 40% in NS5A Tg mice given LPS (Fig. S1), indicating the presence of a major non-Kupffer cell source of TLR4 activation and TNF-α expression in NS5A Tg mice. This conclusion and its relevance to humans are also supported by immunohistochemical colocalization of TLR4 with *p*-JNK and *p*-IκBα in the liver parenchyma of HCV patients. Indeed, this new paradigm offers a logical explanation for a clinical observation that hepatocytes are positively stained for proinflammatory gene expression in HCV patients (35).

Nanog transduction alone is not as effective as TLR4 activation in liver tumorigenesis, as shown by our cell transplantation exper-

iment. We believe that TLR4 activation induces other tumor-driver genes, which cooperatively work with Nanog to cause liver oncogenesis. Thus, Nanog is still essential for TLR4-dependent oncogenesis, but it alone is poorly oncogenic. In our previous work using the Huh7 cell line, we demonstrated that TLR4 promoter upregulation by NS5A is mediated by PU.1, Oct-1, and AP-1 elements (22). The similar transcriptional mechanism may underlie TLR4 induction in primary hepatocytes. Obviously, our future study will need to address this possibility.

The roles of JNK and IKK in liver oncogenesis are important questions. AP-1 is activated in both HCC and chronic hepatitis (32). In vitro studies using liver-derived cell lines demonstrate rapid activation of AP-1 by HBV or HCV proteins (33). Our study also shows activation of JNK in alcohol-fed NS5A Tg mice in concurrence with the increased risk of liver tumors (Fig. S4). Our study did not address which isoform of JNK (JNK1/2) is responsible for NS5A-TLR4-mediated liver damage and oncogenesis, and this is an obvious question that will need to be addressed by our future study.

In summary, the present study has demonstrated that alcohol and HCV NS5A induce synergistic liver tumor development via induction and activation of TLR4 in mice. The importance of Nanog as a direct downstream gene of TLR4 in this oncogenesis has also been identified. These findings indicate that pharmacologic inhibition of TLR4 signaling may provide a novel therapeutic option for HCV-associated liver tumors.

Materials and Methods

Mice. Mice expressing the HCV NS5A gene under control of the apoE promoter were obtained from Ratna Ray at Saint Louis University (St. Louis, MO). NS5A Tg (FVB strain) and Tlr4$^{-/-}$ mice on C57BL/6 strain (Jackson Laboratories) were intercrossed more than 8 generations to produce WT, NS5A, Tlr4$^{-/-}$, and Tlr4$^{-/-}$–NS5A mice on a more congenic genetic background. Tsukamoto-French intragastric ethanol infusion model was applied as previously described (34). Lieber–DeCarli diet containing 3.5% ethanol or isocaloric dextrin (Bioserv) was fed for long-term alcohol feeding. All animal experiments were performed with age- and sex-matched mice from same littermates and conducted in accordance with the approved Institutional Animal Care and Use Committee protocol at the University of Southern California.

Hepatic Progenitor Cell Transduction and Transplantation Experiment. Hepatoblast transplantation experiments were performed by using the protocol previously described for isolation, culture, retroviral/lentiviral infection, and transplantation via spleen of purified *p53*$^{-/-}$ hepatoblasts (1×10^6 cells), as well as retrosine and CCl_4 treatment and tumor monitoring of recipient C57BL/6 mice (31). Tumor volume (cm^3) was calculated by the 3-dimensional animal imaging system at the University of Southern California Molecular Imaging Center. For nude mouse transplantation, Matrigel beads (Invitrogen) were used to anchor hepatoblasts (2×10^6 cells) for s.c. injection.

ACKNOWLEDGMENTS. We thank Qing-gao Deng, Jiaohong Wang, Sean Vorah, and Jeffrey Huang (University of Southern California) for mouse experiments; Michael Karin (University of California at San Diego) for discussions; Paul Robson (Genome Institute of Singapore, Immunos, Singapore) for Nanog-promoter luciferase construct; Steven Weinman (University of Texas) for suggestions; and Moli Chen and Alex Trana for histological service. The study was supported by pilot project funding; the Animal and Morphology Cores of the Southern California Research Center for ALPD & Cirrhosis (P50 AA011999) funded by the National Institute on Alcohol Abuse and Alcoholism/National Institutes of Health (NIAAA/NIH); NIH Grants AI 40038, CA123328, and CA108302; and the Medical Research Service of the Veterans Administration.

1. Okuda K (2000) Hepatocellular carcinoma. *J Hepatol* 32:225–237.
2. Okuda MK, *et al.* (2002) Mitochondrial injury, oxidative stress, and antioxidant gene expression are induced by hepatitis C virus core protein. *Gastroenterology* 122:366–375.
3. Yao F, Terrault N (2001) Hepatitis C and hepatocellular carcinoma. *Curr Treat Options Oncol* 2:473–483.
4. Heintges T, Wands JR (1997) Hepatitis C virus: Epidemiology and transmission. *Hepatology* 26:521–526.
5. Brechot C, Nalpas B, Feitelson MA (1996) Interactions between alcohol and hepatitis viruses in the liver. *Clin Lab Med* 16:273–287.
6. Oshita M, *et al.* (1994) Increased serum hepatitis C virus RNA levels among alcoholic patients with chronic hepatitis C. *Hepatology* 20:1115–1120.
7. Choi J, *et al.* (2004) Reactive oxygen species suppress hepatitis C virus RNA replication in human hepatoma cells. *Hepatology* 39:81–89.
8. Sawada M, Takada A, Takase S, Takada N (1993) Effects of alcohol on the replication of hepatitis C virus. *Alcohol Alcohol Suppl* 1B:85–90.
9. Izzotti A, *et al.* (1998) DNA alterations in rat organs after chronic exposure to cigarette smoke and/or ethanol ingestion. *FASEB J* 12:753–758.
10. Moriya K, *et al.* (2001) Oxidative stress in the absence of inflammation in a mouse model for hepatitis C virus-associated hepatocarcinogenesis. *Cancer Res* 61:4365–4370.
11. Perlemuter G, *et al.* (2002) Hepatitis C virus core protein inhibits microsomal triglyceride transfer protein activity and very low density lipoprotein secretion: A model of viral-related steatosis. *FASEB J* 16:185–194.
12. Kawaguchi T, *et al.* (2004) Hepatitis C virus down-regulates insulin receptor substrates 1 and 2 through up-regulation of suppressor of cytokine signaling 3. *Am J Pathol* 165:1499–1508.
13. Banerjee S, *et al.* (2008) Hepatitis C virus core protein upregulates serine phosphorylation of insulin receptor substrate-1 and impairs the downstream akt/protein kinase B signaling pathway for insulin resistance. *J Virol* 82:2606–2612.
14. Koike K, *et al.* (2008) Molecular basis for the synergy between alcohol and hepatitis C virus in hepatocarcinogenesis. *J Gastroenterol Hepatol* 23(Suppl 1):S87–S91.
15. Donato F, Gelatti U, Limina RM, Fattovich G (2006) Southern Europe as an example of interaction between various environmental factors: A systematic review of the epidemiologic evidence. *Oncogene* 25:3756–3770.
16. Hassan MM, *et al.* (2002) Risk factors for hepatocellular carcinoma: Synergism of alcohol with viral hepatitis and diabetes mellitus. *Hepatology* 36:1206–1213.
17. Lai MS, Hsieh MS, Chiu YH, Chen TH (2006) Type 2 diabetes and hepatocellular carcinoma: A cohort study in high prevalence area of hepatitis virus infection. *Hepatology* 43:1295–1302.
18. Peters MG, Terrault NA (2002) Alcohol use and hepatitis C. *Hepatology* 36:S220–S225.
19. Yuan JM, Govindarajan S, Arakawa K, Yu MC (2004) Synergism of alcohol, diabetes, and viral hepatitis on the risk of hepatocellular carcinoma in blacks and whites in the U.S. *Cancer* 101:1009–1017.
20. Kato N, Lan NH, Ono-Nita SK, Shiratori Y, Omata M (1997) Hepatitis C virus nonstructural region 5A protein is a potent transcriptional activator. *J Virol* 71:8856–8859.
21. Gale MJ, Jr, *et al.* (1997) Evidence that hepatitis C virus resistance to interferon is mediated through repression of the PKR protein kinase by the nonstructural 5A protein. *Virology* 230:217–227.
22. Machida K, *et al.* (2006) Hepatitis C virus induces toll-like receptor 4 expression, leading to enhanced production of beta interferon and interleukin-6. *J Virol* 80:866–874.
23. Majumder M, *et al.* (2003) Expression of hepatitis C virus non-structural 5A protein in the liver of transgenic mice. *FEBS Lett* 555:528–532.
24. Majumder M, *et al.* (2002) Hepatitis C virus NS5A protein impairs TNF-mediated hepatic apoptosis, but not by an anti-FAS antibody, in transgenic mice. *Virology* 294:94–105.
25. Kurata K, *et al.* (2008) Stress via p53 pathway causes apoptosis by mitochondrial Noxa upregulation in doxorubicin-treated neuroblastoma cells. *Oncogene* 27:741–754.
26. Li J, Lee B, Lee AS (2006) Endoplasmic reticulum stress-induced apoptosis: Multiple pathways and activation of p53-up-regulated modulator of apoptosis (PUMA) and NOXA by p53. *J Biol Chem* 281:7260–7270.
27. Van Rooijen N, Kors N, vd Ende M, Dijkstra CD (1990) Depletion and repopulation of macrophages in spleen and liver of rat after intravenous treatment with liposome-encapsulated dichloromethylene diphosphonate. *Cell Tissue Res* 260:215–222.
28. Wu D, Cederbaum A (2008) Cytochrome P4502E1 sensitizes to tumor necrosis factor alpha-induced liver injury through activation of mitogen-activated protein kinases in mice. *Hepatology* 47:1005–1017.
29. Lu Y, Zhuge J, Wang X, Bai J, Cederbaum AI (2008) Cytochrome P450 2E1 contributes to ethanol-induced fatty liver in mice. *Hepatology* 47:1483–1494.
30. Lee JS, *et al.* (2006) A novel prognostic subtype of human hepatocellular carcinoma derived from hepatic progenitor cells. *Nat Med* 12:410–416.
31. Zender L, *et al.* (2006) Identification and validation of oncogenes in liver cancer using an integrative oncogenomic approach. *Cell* 125:1253–1267.
32. Liu P, *et al.* (2002) Activation of NF-kappa B, AP-1 and STAT transcription factors is a frequent and early event in human hepatocellular carcinomas. *J Hepatol* 37:63–71.
33. Kato N, *et al.* (2000) Activation of intracellular signaling by hepatitis B and C viruses: C-viral core is the most potent signal inducer. *Hepatology* 32:405–412.
34. Tsukamoto H, Towner SJ, Ciofalo LM, French SW (1986) Ethanol-induced liver fibrosis in rats fed high fat diet. *Hepatology* 6:814–822.